A Role for the Insulin Receptor in the Suppression of Dengue Virus and Zika Virus in Wolbachia-Infected Mosquito Cells

Gholamreza Haqshenas, Gerard Terradas, Prasad N. Paradkar, Jean-Bernard Duchemin, Elizabeth A. Mcgraw, Christian Doerig

Cell Reports

A Role for the Insulin Receptor in the Suppression of Dengue Virus and Zika Virus in *Wolbachia*-Infected Mosquito Cells

Graphical Abstract

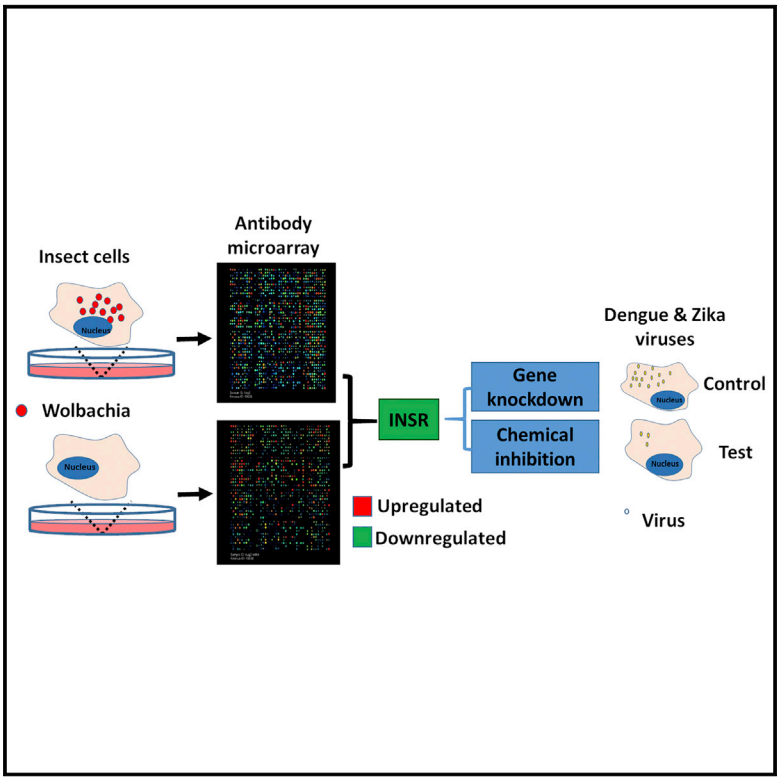

Highlights

- Antibody microarray to investigate mosquito host cell signaling response to *Wolbachia*
- *Wolbachia*-infected cells show downregulation of the host cell insulin receptor (IR)
- Inhibition or silencing of IR impairs the replication of dengue and Zika viruses *in vitro*
- Mosquitoes fed the IR inhibitor have impaired Zika virus replication

Authors

Gholamreza Haqshenas, Gerard Terradas, Prasad N. Paradkar, Jean-Bernard Duchemin, Elizabeth A. McGraw, Christian Doerig

Correspondence

gholamreza.haqshenas@monash.edu (G.H.), eam7@psu.edu (E.A.M.), christian.doerig@rmit.edu.au (C.D.)

In Brief

Wolbachia-infected mosquitoes are deployed in tropical regions to combat arbovirus transmission. However, the mechanism of superinfection blocking is unknown. Haqshenas et al. show that *Wolbachia* downregulates the mosquito's insulin receptor. Knockdown or inhibition of the mosquito's insulin receptor recapitulates the block of viral infection caused by *Wolbachia*.

Haqshenas et al., 2019, Cell Reports *26*, 529–535
January 15, 2019
https://doi.org/10.1016/j.celrep.2018.12.068

CellPress

Cell Reports
Report

A Role for the Insulin Receptor in the Suppression of Dengue Virus and Zika Virus in *Wolbachia*-Infected Mosquito Cells

Gholamreza Haqshenas,[1,*] Gerard Terradas,[2] Prasad N. Paradkar,[3] Jean-Bernard Duchemin,[3] Elizabeth A. McGraw,[2,4,*] and Christian Doerig[1,5,6,*]

[1]Infection and Immunity Program, Monash Biomedicine Discovery Institute and Department of Microbiology, Monash University, Clayton, VIC 3800, Australia
[2]School of Biological Sciences, Monash University, Clayton, VIC 3800, Australia
[3]CSIRO Health and Biosecurity, Australian Animal Health Laboratory, Geelong, VIC, Australia
[4]Department of Entomology, Center for Infectious Disease Dynamics, Pennsylvania State University, University Park, PA 16802, USA
[5]Present address: School of Health and Biomedical Sciences, RMIT University, Bundoora, VIC 3083, Australia
[6]Lead Contact
*Correspondence: gholamreza.haqshenas@monash.edu (G.H.), eam7@psu.edu (E.A.M.), christian.doerig@rmit.edu.au (C.D.)
https://doi.org/10.1016/j.celrep.2018.12.068

SUMMARY

***Wolbachia*-infected mosquitoes are refractory to super-infection with arthropod-borne pathogens, but the role of host cell signaling proteins in pathogen-blocking mechanisms remains to be elucidated. Here, we use an antibody microarray approach to provide a comprehensive picture of the signaling response of *Aedes aegypti*-derived cells to *Wolbachia*. This approach identifies the host cell insulin receptor as being downregulated by the bacterium. Furthermore, siRNA-mediated knockdown and treatment with a small-molecule inhibitor of the insulin receptor kinase concur to assign a crucial role for this enzyme in the replication of dengue and Zika viruses in cultured mosquito cells. Finally, we show that the production of Zika virus in *Wolbachia*-free live mosquitoes is impaired by treatment with the selective inhibitor mimicking *Wolbachia* infection. This study identifies *Wolbachia*-mediated downregulation of insulin receptor kinase activity as a mechanism contributing to the blocking of super-infection by arboviruses.**

INTRODUCTION

Wolbachia pipientis is an obligate intracellular endosymbiotic bacterium that naturally infects many arthropod species. However, many of the world's most important mosquito vectors, including some (Bian et al., 2013a) but not all (Shaw et al., 2016) of the *Anopheles* species that transmit malaria parasites, as well as *Aedes aegypti*, which transmits dengue virus (DENV), Zika virus (ZIKV), yellow fever, and Chikungunya (CHIK) virus, among others, are naturally *Wolbachia*-free (McMeniman et al., 2009). Transinfection approaches have been used to create stably inherited *Wolbachia* infections in *Ae. aegypti* (McMeniman et al., 2009; Walker et al., 2011). In these artificially infected mosquito hosts (Bian et al., 2013a; Kambris et al., 2009; Moreira et al., 2009; van den Hurk et al., 2012; Ye et al., 2013) and in a range of naturally infected insects (Bian et al., 2013b; Hedges et al., 2008; Moreira et al., 2009; Ye et al., 2013), *Wolbachia* infection has been shown to limit the replication of co-infecting bacteria, viruses, fungi, and parasites. This pathogen-blocking ability forms the cornerstone of a global initiative to trial the use of *Wolbachia* for reducing the incidence of vector-borne diseases via limiting mosquito transmission of pathogens, notably DENV and ZIKV (Aliota et al., 2016; Frentiu et al., 2010; Moreira et al., 2009), by *Ae. aegypti* populations. Despite deployment of *Wolbachia*-infected mosquitoes at an increasing number of field sites (O'Neill, 2018), the mechanism(s) of *Wolbachia*-mediated pathogen blocking remain(s) to be fully elucidated (Terradas and McGraw, 2017). Recently, we have demonstrated that the signalome-wide response to intracellular pathogens can be assessed using a combination of antibody microarrays comprising pan- and phosphospecific antibodies against host cell signaling molecules and functional validation of hits by small interfering RNA (siRNA) (Haqshenas et al., 2017). Here we deployed this strategy to characterize the signaling response of *Ae. aegypti* cells to *Wolbachia* infection and discovered that the phosphorylation status of the insulin receptor in the *Ae. aegypti* host cell is affected by *Wolbachia* infection. We show that replication of both DENV and ZIKV is impaired by siRNA knockdown of the insulin receptor (IR, a receptor tyrosine kinase) in mosquito cells and that treatment with a selective small-molecule inhibitor of the IR kinase activity drastically reduces virus replication in both *Ae aegypti*-derived cells and live mosquitoes.

RESULTS

Antibody Array Profiling of Mosquito Cell Response to Wolbachia Infection

We used the Kinexus antibody microarray to compare signaling pathways active in *Wolbachia*-infected cells with those in *Wolbachia*-free cells. The microarray comprises 895 antibodies against human signalome components, including 265 pan-specific antibodies against their target proteins (allowing comparison of

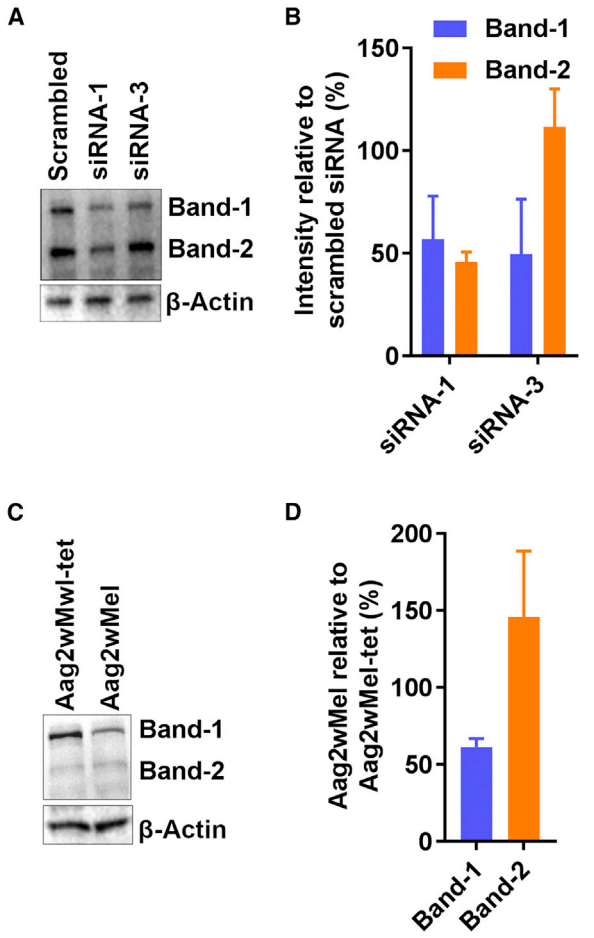

Figure 1. Immunoblot Analysis of the Insulin Receptor (IR) in *Wolbachia*-Infected Mosquito Cells (Aag2wMel) or Non-infected (Aag2w-Mel-tet) Cells

(A) Representative immunoblot of 3 replicates of Aag2wMel-tet cells that were transfected with siRNA-1 and siRNA-3 targeting IR transcripts. A scrambled RNA was used as a control. The IR was detected with a phosphosite-specific antibody against human IR pY1189.

(B) The intensity of putative IR protein bands (bands 1 and 2) of three replicates were measured and normalized to actin. The bars represent SD.

(C) Aag2wMel and Aag2wMel-tet cells were seeded in a 48-well plate and directly lysed using the same amounts of Laemmli buffer after 5 days of incubation. 20 μL was loaded onto a precast acrylamide gel (STAR Methods), and the IR was detected as described for Figure 2A.

(D) The intensity of putative IR protein bands (bands 1 and 2) of three replicates were measured and normalized to actin. The bars represent SD. The HiMark Pre-Stained Protein Standard was used as the protein size marker.

protein abundance between the two samples irrespective of their phosphorylation status) and 613 phospho-specific antibodies (allowing comparison of the occupancy status of specific phosphosites). Because the core components of many signaling pathways, and in particular those mediating phosphorylation-dependent regulation, are evolutionarily highly conserved across metazoans (and beyond), we reasoned that many antibodies on the array would recognize mosquito signaling proteins and their regulatory phosphosites. Indeed, the alignment of amino acid sequences of signaling proteins revealed that many are highly conserved in the antibody recognition epitope between humans and mosquitoes, as exemplified in Figure S1. We therefore set out to interrogate the signalome of *Wolbachia*-infected versus non-infected *Ae. aegypti* cells. The array did indeed provide useful information; we found that the expression and/or phosphorylation status of 117 cell factors was significantly different between *Wolbachia*-infected and *Wolbachia*-free samples. The signal yielded by 77 antibodies (49 pan-specific and 28 phospho-specific) was upregulated, and the signal yielded by 64 antibodies (6 pan-specific and 58 phospho-specific) was downregulated; 4 were upregulated in total protein level but downregulated in their phosphorylated status (Table S1). Overall, the dataset reveals that *Wolbachia* infection results in the modulation of individual signaling pathways (e.g., mitogen-activated protein kinase [MAPK] pathways), cellular functions such as translation, and cell cycle progression because of space constraints; a detailed description of the affected pathways will be published elsewhere. Here we focus on the downregulation of both the abundance and phosphorylation level of the insulin receptor in *Wolbachia*-infected cells.

The IR Plays an Important Role in Virus Replication in Mosquito Cells

Both the abundance of the IR and the occupancy of its activating phosphorylation sites (pY1189 and pY1189-pY1190) are downregulated by 47%, 62%, and 59%, respectively, in response to *Wolbachia* infection. Alignment of human and *Ae. aegypti* IR amino acid sequences revealed that the epitope detected in the Kinexus microarray is conserved between humans and mosquitoes (Figure S1). Unfortunately, IR substrate 1 (IRS1), a major immediate substrate of the IR kinase in mammalian cells against which a phospho-specific antibody is present on the array, is not conserved in *Ae. aegypti*.

Interestingly, the IR has recently been shown to be required for DENV replication in mammalian cells (Kumar et al., 2016). The decrease in both abundance and phosphorylation levels of IR in *Wolbachia*-positive mosquito cells might contribute to the block of DENV and ZIKV replication in *Wolbachia*-infected mosquitoes (Caragata et al., 2016). To test this hypothesis, we investigated the role of this receptor tyrosine kinase in the replication of ZIKV and DENV in *Ae. aegypti* cells. We designed three different siRNAs against the IR (Table S1) within exon 16 (siRNA-1 and siRNA-2) and exon 3 (siRNA-3) of the IR transcript and tested them in a time course study. The *Ae. aegypti* IR gene comprises 16 exons (VectorBase: AAEL002317). All three siRNAs reduced DENV replication in *Wolbachia*-free cells; of these, siRNA-1 displayed the highest suppressive effect on virus replication (Figure S2). Subsequently, we assessed the effect of siRNA-1 and 3 on IR silencing using the Kinexus IR phosphosite-specific antibody in western blot analyses. This antibody recognizes pY1189 of the human IR (short-listed for further analysis; Table S1), which is highly conserved between humans and *Ae. aegypti* (Figure S1). Using the anti-pY1189 antibody, we detected at least two protein bands with approximate sizes of 150 and 360 kDa whose quantities were reduced when *Wolbachia*-free cells were treated with siRNAs 1 and 3 (Figures 1A and 1B). siRNA-1, targeting exon 16, reduced the abundance

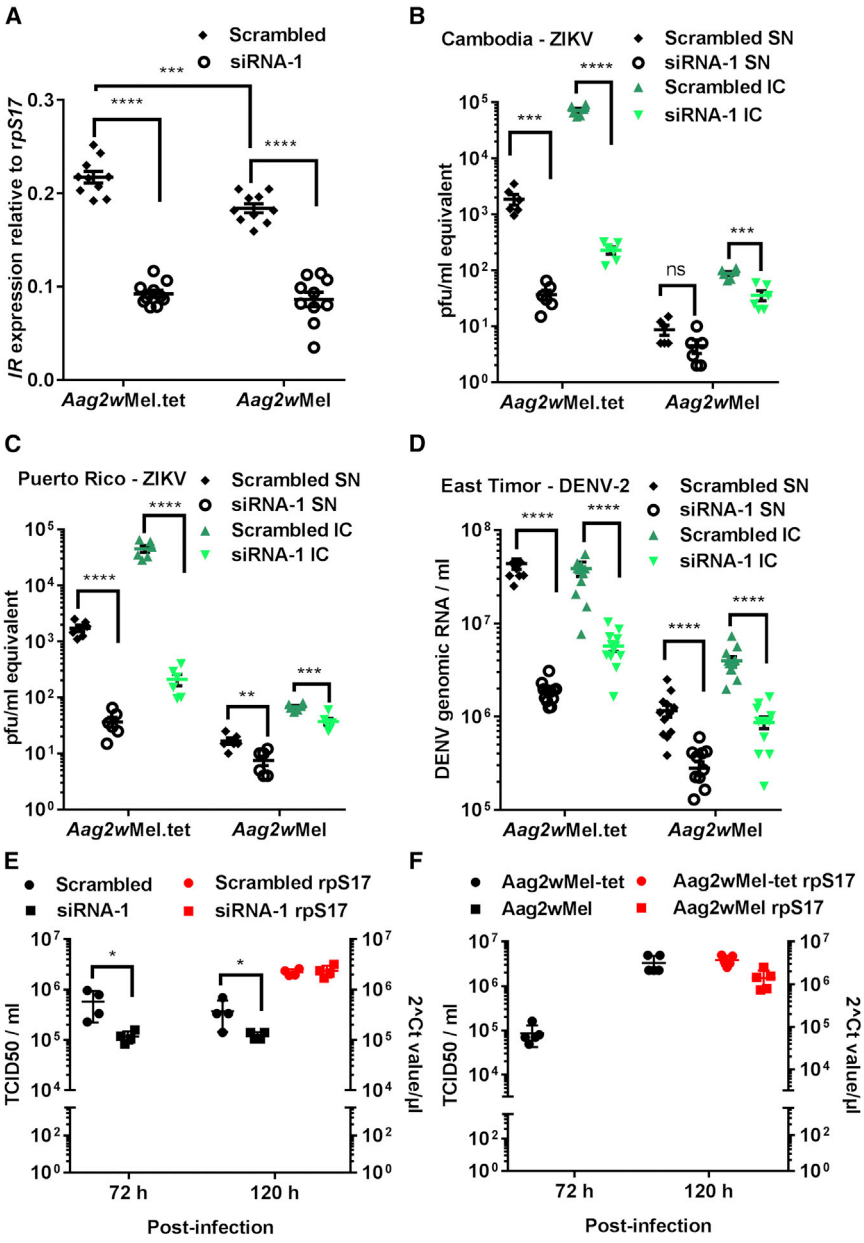

Figure 2. Role of the Insulin Receptor (IR) in Zika Virus and Dengue Virus Replication

(A) The IR gene was knocked down by specific siRNA in *Wolbachia*-infected and non-infected cells, and the level of knockdown was evaluated by RT-PCR normalized to the *Ae. aegypti* housekeeping gene rpS17.

(B–D) The cells were subsequently infected with ZIKV (strains Cambodia 2010 and Puerto Rico 2016) (B and C) and DENV-2 (D) at MOI 0.1 and 0.5, respectively. Viral RNA was quantified in culture supernatants and in cell lysates 5 days post-infection and normalized to *Ae. aegypti* housekeeping gene rpS17. IC, intracellular viral RNA; SN, viral RNA in the supernatant fluid. Average values (n = 10 per treatment) are shown on the graphs, and the bars represent SD. Significance is based on Student's t test on data. *p < 0.05, **p < 0.01, ***p < 0.001, ****p < 0001.

(E and F) The effect of IR silencing (E) and *Wolbachia* infection (F) on infectious DENV production (5 replicates). The virus titer 24 h post-infection was below the detection level (100 50 percent tissue culture infectious dose [TCID50]/mL). *Wolbachia*-infected cells produced less than 100 TCID50/mL. The rpS17 gene levels were measured by qPCR, and the square power of the obtained cycle threshold (Ct) values were plotted against the right axis. Bars represent SD.

of both protein bands, whereas siRNA-3, targeting exon 3, reduced the quantity of the 360-kDa band only, suggesting that the 150-kDa protein band represents an IR variant lacking exon 3. The 360-kDa protein band was also suppressed by ~40% in *Wolbachia*-infected cells (Figures 1B and 1C). Selective silencing of the IR gene was verified by qRT-PCR using forward and reverse oligonucleotides within exons 9 and 10 of the IR gene, respectively, and mRNA levels were normalized to the host cell rpS17 gene copy number (Figure 2A). Consistent with the microarray results, Figure 2A shows a decrease in the IR transcripts of *Wolbachia*-infected cells. To test the role of the IR in ZIKV replication, we first established an *in vitro* system for the infection of *Wolbachia*-infected mosquito cells with ZIKV. We infected *Wolbachia*-infected *Ae. aegypti* cells with two strains of ZIKV, Cambodia 2010 and Puerto Rico 2016, using MOI values of 10, 1, 0.1, and 0.01. The presence of *Wolbachia* reduced virus replication, the highest effect being observed when an MOI of 0.1 was used for viral infection (Figure S3).

We then used the ZIKV and DENV cell culture systems to assess whether the downregulation of IR in *Wolbachia*-infected cells is implicated in the suppression of ZIKV and DENV replication. Consistent with published reports indicating that knockdown of IR reduced DENV replication in mammalian cells (Kumar et al., 2016), IR silencing suppressed ZIKV and DENV replication in both *Wolbachia*-infected and *Wolbachia*-free mosquito cells (Figures 2B–2D); the effect was more prominent in *Wolbachia*-free cells, which is not surprising because the levels of the IR are lower in the presence of *Wolbachia* (see above). Silencing the IR gene in *Wolbachia*-free cells recapitulated the effect of *Wolbachia* infection with respect to super-infection with both arboviruses. The qRT-PCR results were validated by measurement of the effects of siRNA-1 on the secretion of infectious DENV into the supernatant fluid (Figure 2E). The effect of downregulation of the IR by siRNA on virus production was not as strong as that observed upon *Wolbachia* infection (Figures 2E and 2F). We then used a selective chemical kinase inhibitor of the IR, hydroxy-2-naphthalenyl-methyl

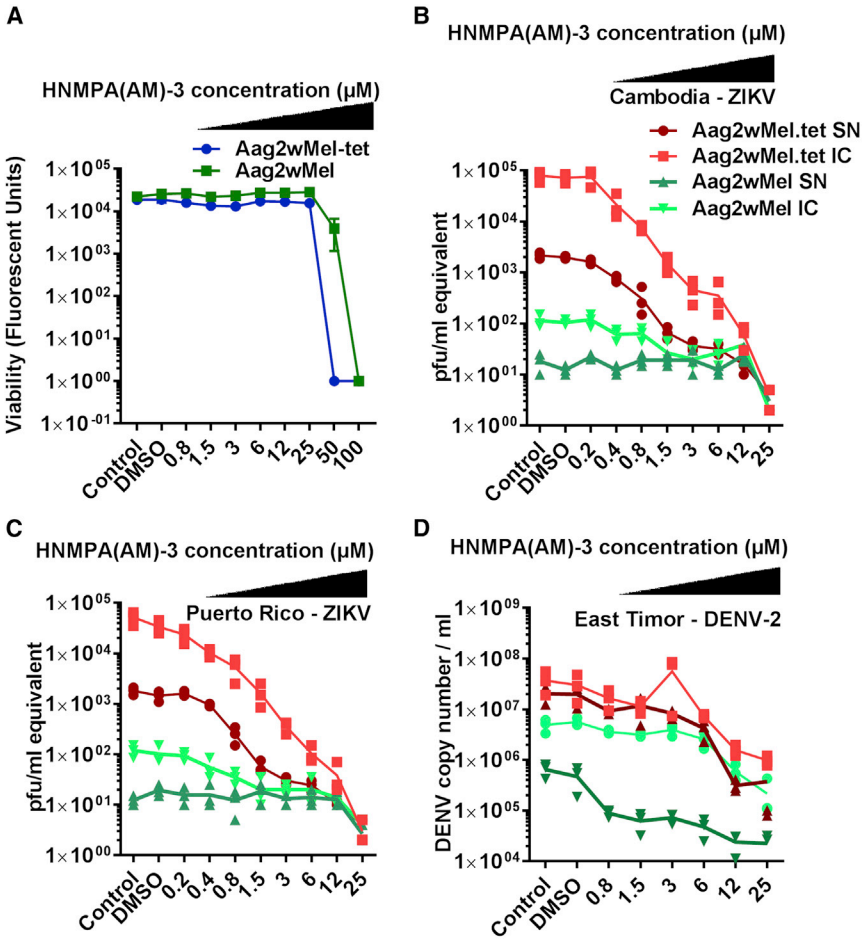

Figure 3. Effects of HNMPA(AM)-3, a Selective Insulin Receptor Inhibitor, on Replication of Zika Virus and Dengue Virus

(A) The toxicity of the compound for Aag2*w*Mel and Aag2*w*Mel.tet cells (6 replicates) was tested 5 days after treatment with different concentrations of the compound using PrestoBlue cell viability reagent (Thermo Fisher Scientific).

(B–D) Subsequently, the effect of the compound on the replication of two strains of Zika virus (Cambodia 2010, B; Puerto Rico 2016, C) and of DENV-2 (D) was determined as described in the STAR Methods. Viral RNA, extracted from supernatant fluids and cell lysate samples, was quantified by qRT-PCR and normalized to the *Ae. aegypti* housekeeping gene rpS17.

Experiments were performed in triplicate for each compound concentration. Bars represent SD.

phosphonic acid trisacetoxymethylester (HNMPA(AM)-3) (Fan et al., 2016), to determine whether IR kinase activity is required for ZIKV and DENV replication. Cell toxicity assays revealed that concentrations $\leq$ 25 μM of the inhibitor are non-toxic for *Wolbachia*-infected (Aag2*w*Mel) and non-infected (Aag2*w*Mel.tet) cells (Figure 3A). Using a range of inhibitor concentrations (0.2 to 25 μM), we determined that HNMPA(AM)-3 inhibited both ZIKV strains and DENV-2 in a dose-dependent manner (Figures 3B–3D). Treatment with the IR inhibitor reduced ZIKV and DENV RNA in both the supernatant fluid and cell lysates; the effect was more pronounced for ZIKV (Figures 3B and 3C) than for DENV (Figure 3D), but clear inhibition was evident with both viruses. This suggests that IR kinase activity is essential for replication of both ZIKV and DENV in mosquito cells, and its downregulation by *Wolbachia* provides a putative contributing mechanism for blocking of secondary infections.

Treatment with an Inhibitor of IR Activity Impairs ZIKV Replication in Live Mosquitoes

Following demonstration of the importance of the IR for replication of DENV and ZIKV in mosquito cells *in vitro*, we tested whether the IR inhibitor impairs ZIKV replication in live mosquitoes. Two strains of *Ae. aegypti* mosquitoes, Brisbane and Higgs, were fed with 12 μM HNMPA(AM)-3 (a concentration that suppressed ZIKV replication in cultured cells and was non-toxic for cultured mosquito cells; see above) and infected with ZIKV (Cambodia 2010 strain) in the blood meal at a final concentration of 10^5 plaque-forming units (PFU)/mL. Seven days after infection, total RNA was extracted from entire carcasses and from dissected midguts, and viral RNA was measured by qRT-PCR and normalized to a housekeeping gene mRNA as described above. As shown in Figure 4, treatment of both mosquito strains with the inhibitor, compared with treatment with the carrier (DMSO) alone, reduced virus replication by approximately 2 logs in carcasses and midguts ($p < 0.0001$).

DISCUSSION

The bacterial endosymbiont *Wolbachia* can infect a wide range of insects, including *Ae. aegypti,* the vector of many major human pathogens such as ZIKV and DENV. Here we used a comprehensive microarray of antibodies directed against hundreds of signaling proteins and their phosphorylation sites to characterize the insect cell signaling response to *Wolbachia*. This approach revealed downregulation of IR abundance and phosphorylation levels in infected cells. Subsequent characterization of the role of the IR in ZIKV and DENV replication using siRNA and pharmacological approaches confirmed that IR suppression by *Wolbachia*, as detected by microarray, quantifcation of transcipts, and western blot analyses, contributes to the mechanisms by which the bacterium suppresses secondary infection with viruses. Although off-target effects of the siRNAs and IR inhibitor cannot be formally excluded, the fact that both recapitulate the *Wolbachia*-based viral suppression phenotype strongly suggest that a functioning IR receptor kinase is required

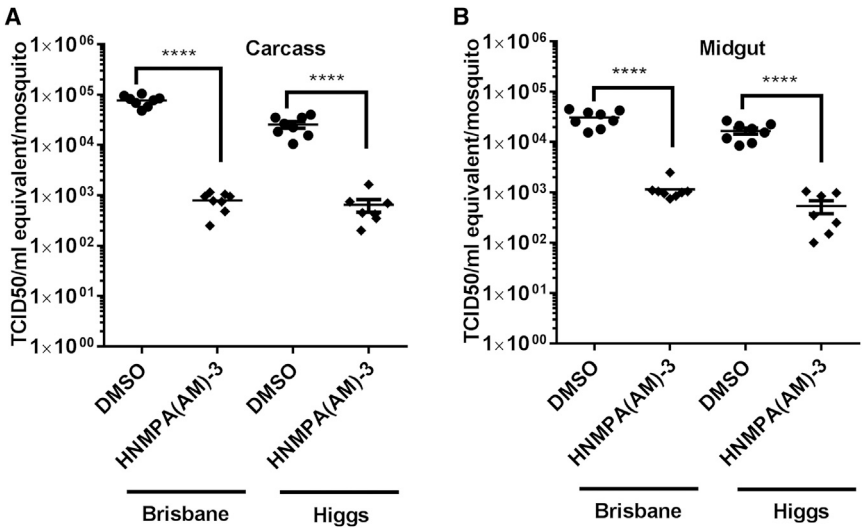

Figure 4. Effects of HNMPA(AM)-3, a Selective Inhibitor of the Insulin Receptor, on Zika Virus Replication in Live Mosquitoes

(A and B) Two different strains of *Ae. aegypti* mosquitoes, one from Australia (Brisbane strain) and the other from the United States (Higgs strain). Mosquitoes were infected with Zika virus (Cambodia 2010 strain) with or without HNMPA(AM)-3 (12 μM) in the same blood meal. Blood-fed mosquitoes were selected and, 7 days later, dissected for carcass (A) and midgut (B). Real-time RT-PCR was performed using Zika virus-specific primers, and the data were normalized using the housekeeping gene rpS17. The TCID50/mL equivalent was calculated as described in the STAR Methods. Averages (n = 7–8 per treatment) are shown on the graphs, and the bars represent SD. The statistical significance is based on a Student's t test. ****p < 0001.

for viral infection in these cells. Together with the microarray as well as transcript quatification and western blot data regarding the effects of *Wolbachia* infection, these observations implicate the IR as a contributor to the suppression of viral super-infection in *Wolbachia*-infected cells.

The human IR precursor and its various isoforms display 210-, 135-, and 95-kDa apparent molecular masses (Kasuga et al., 1982). Bioinformatic analysis of the *Ae. aegypti* genome (VectorBase public domain) has identified two potential IR mRNAs (AAEL002317) that encode potential proteins of 1,590 and 1,814 amino acids, with predicted molecular masses of ~175 and ~200 kDa, respectively. Our western blot data (Figure 1) display two bands with molecular masses of 150 and 360 kDa (one report suggests that the mosquito IR migrates at an approximate size of 500 kDa [Wen et al., 2010], but the antibody used in that study is not available commercially). Further comprehensive experimental studies are required to explain the discrepancy between bioinformatics and experimental data. Our microarray and western analyses concur to demonstrate that *Wolbachia* reduces IR phosphorylation, and, hence, most presumably, kinase activity. Interestingly, cholesterol levels, which are reduced in *Wolbachia*-infected mosquitoes (Caragata et al., 2013) and *Wolbachia*-infected cultured mosquito cells (Molloy et al., 2016), play a regulatory role in the stimulation of IR-mediated signaling pathways; cholesterol depletion, although not affecting IR stability or autophosphorylation activity, the pathway lying downstream of IR, which involves IRS-1 (insulin receptor substrate 1) and AKT-PKB (Adachi et al., 2002; Gustavsson et al., 1999; Parpal et al., 2001; Vainio et al., 2002). *Wolbachia* requires lipids from its host cell (Wu et al., 2004), which may therefore become scarce during symbiont infection. A recent study demonstrated that *Wolbachia* induces accumulation of cellular esterified cholesterol in lipid droplets, perturbing cholesterol homeostasis (Geoghegan et al., 2017). The impairment of cholesterol homeostasis and, consequently, the possible perturbation of IR-mediated signal transduction in *Wolbachia*-infected cells may explain our observations that IR silencing or chemical inhibition resulted in a less noticeable effect on replication of ZIKV and DENV in *Wolbachia*-infected cells than in non-infected cells. In line with our observations in mosquito cells, an siRNA screen demonstrated that the IR is essential for DENV replication in mammalian cells (Kumar et al., 2016), although its role in the DENV life cycle in mammalian cells remains to be clarified. The potency of the IR-selective inhibitor HNMPA(AM)-3 was higher in insect than in mammalian cells. In contrast to our results using *Ae. aegypti* cells, a previous report indicated that removal of *Wolbachia* from *Drosophila* enhances the phenotype of mutants that are impaired in the insulin pathway, suggesting that *Wolbachia* normally acts to increase insulin signaling in *Drosophila* (Ikeya et al., 2009). A possible explanation for this discrepancy may be that *Ae. Aegypti*, unlike *Drosophila*, is not a natural host for *Wolbachia*. It would be of great interest to implement the antibody microarray approach to investigate the *Drosophila's* response to *Wolbachia* infection.

Additional mechanisms for the pathogen-blocking phenotype of *Wolbachia*-infected cells have been proposed recently. Overexpression of the Mt2 methyltransferase (Bhattacharya et al., 2017) and of the Vago1 protein (Asad et al., 2018a), inhibition of the West Nile virus (WNV)-mediated XRN1 activity blockage (Thomas et al., 2018), suppression of *Aedes* chromodomain helicase DNA binding protein 7 (AeCHD7) (Asad et al., 2016) and of the pelo protein (Asad et al., 2018b), and translation inhibition (Schultz et al., 2018) have all been implicated in the suppression of arbovirus super-infection. Interestingly, several hits from our antibody microarray analysis pertain to signaling pathways that may be highly relevant to at least some of these proposed mechanisms (Table S1) and provide interesting testable hypotheses. As mentioned above, these data will be discussed elsewhere.

In brief, our study indicates that downregulation of IR signaling is a mechanism contributing to the blocking of secondary viral infections in *Wolbachia*-positive cells and provides initial insights into signaling pathways pertaining to parallel mechanisms that underlie this phenomenon.

STAR★METHODS

Detailed methods are provided in the online version of this paper and include the following:

- KEY RESOURCES TABLE
- CONTACT FOR REAGENT AND RESOURCE SHARING
- EXPERIMENTAL MODEL AND SUBJECT DETAILS
  - Mosquito cell lines
  - Mosquitoes
- METHOD DETAILS
  - Kinexus™ antibody microarray
  - Selection of candidate genes and their targeting with siRNA and small molecules
  - Infection of live mosquitoes with ZIKV and treatment with the IR inhibitor
  - siRNA transfection
  - Immunoblot analysis
  - DENV and ZIKV infection and quantification
- DATA ANALYSIS
- QUANTIFICATION AND STATISTICAL ANALYSIS

SUPPLEMENTAL INFORMATION

Supplemental Information includes four figures and two tables and can be found with this article online at https://doi.org/10.1016/j.celrep.2018.12.068.

ACKNOWLEDGMENTS

The research was supported by the C.D. group and NHMRC project grant APP1103804 (to E.M.). The Higgs and Brisbane mosquito lines were gifts from Dr. Akbari (University of California, Riverside) and Dr. Ary Hoffmann (University of Melbourne, Australia), respectively. The authors would like to thank Emily Kerton (Monash University, Australia) for her technical assistance.

AUTHOR CONTRIBUTIONS

G.H. and C.D. designed the project, and G.H. conducted the Kinexus antibody microarray experiments. G.H., G.T., and P.N.P. performed the chemical inhibition and siRNA experiments. P.N.P. and J.-B.D. performed the mosquito experiment and analyzed the data. G.H., C.D., and E.A.M. designed the concept and contributed to data analysis. G.H. wrote the first draft. All authors contributed to the writing of the manuscript.

DECLARATION OF INTERESTS

The authors declare no competing interests.

Received: December 12, 2017
Revised: October 25, 2018
Accepted: December 12, 2018
Published: January 15, 2019

REFERENCES

Adachi, M., Sampath, J., Lan, L.B., Sun, D., Hargrove, P., Flatley, R., Tatum, A., Edwards, M.Z., Wezeman, M., Matherly, L., et al. (2002). Expression of MRP4 confers resistance to ganciclovir and compromises bystander cell killing. J. Biol. Chem. *277*, 38998–39004.

Aliota, M.T., Walker, E.C., Uribe Yepes, A., Velez, I.D., Christensen, B.M., and Osorio, J.E. (2016). The wMel Strain of Wolbachia Reduces Transmission of Chikungunya Virus in Aedes aegypti. PLoS Negl. Trop. Dis. *10*, e0004677.

Asad, S., Hall-Mendelin, S., and Asgari, S. (2016). Downregulation of Aedes aegypti chromodomain helicase DNA binding protein 7/Kismet by Wolbachia and its effect on dengue virus replication. Sci. Rep. *6*, 36850.

Asad, S., Parry, R., and Asgari, S. (2018a). Upregulation of Aedes aegypti Vago1 by Wolbachia and its effect on dengue virus replication. Insect Biochem. Mol. Biol. *92*, 45–52.

Asad, S., Hussain, M., Hugo, L., Osei-Amo, S., Zhang, G., Watterson, D., and Asgari, S. (2018b). Suppression of the pelo protein by Wolbachia and its effect on dengue virus in Aedes aegypti. PLoS Negl. Trop. Dis. *12*, e0006405.

Bhattacharya, T., Newton, I.L.G., and Hardy, R.W. (2017). Wolbachia elevates host methyltransferase expression to block an RNA virus early during infection. PLoS Pathog. *13*, e1006427.

Bian, G., Joshi, D., Dong, Y., Lu, P., Zhou, G., Pan, X., Xu, Y., Dimopoulos, G., and Xi, Z. (2013a). Wolbachia invades Anopheles stephensi populations and induces refractoriness to Plasmodium infection. Science *340*, 748–751.

Bian, G., Zhou, G., Lu, P., and Xi, Z. (2013b). Replacing a native Wolbachia with a novel strain results in an increase in endosymbiont load and resistance to dengue virus in a mosquito vector. PLoS Negl. Trop. Dis. *7*, e2250.

Buchman, A., Gamez, S., Li, M., Antoshechkin, I., Lee, H.-H., Wang, S.-W., Chen, C.-H., Klein, M.J., Duchmemin, J.-B., Paradkar, P.N., and Akbari, O.S. (2018). Engineered resistance to Zika virus in transgenic Ae. Aegypti expressing a polycistronic cluster of of synthetic miRNAs. bioRxiv. https://doi.org/10.1101/344697.

Caragata, E.P., Rancès, E., Hedges, L.M., Gofton, A.W., Johnson, K.N., O'Neill, S.L., and McGraw, E.A. (2013). Dietary cholesterol modulates pathogen blocking by Wolbachia. PLoS Pathog. *9*, e1003459.

Caragata, E.P., Dutra, H.L.C., and Moreira, L.A. (2016). Inhibition of Zika virus by *Wolbachia* in *Aedes aegypti*. Microb. Cell *3*, 293–295.

Duchemin, J.-B., Mee, P.T., Lynch, S.E., Vedururu, R., Trinidad, L., and Paradkar, P. (2017). Zika vector transmission risk in temperate Australia: a vector competence study. Virol. J. *14*, 108.

Fallon, A.M., and Sun, D. (2001). Exploration of mosquito immunity using cells in culture. Insect Biochem. Mol. Biol. *31*, 263–278.

Fan, B.-S., Zhang, E.-H., Wu, M., Guo, J.-M., Su, D.-F., Liu, X., and Yu, J.-G. (2016). Activation of α7 nicotinic acetylcholine receptor decreases on-site mortality in crush syndrome through insulin signaling-Na/K-ATPase pathway. Front. Pharmacol. *7*, 79.

Frentiu, F.D., Robinson, J., Young, P.R., McGraw, E.A., and O'Neill, S.L. (2010). Wolbachia-mediated resistance to dengue virus infection and death at the cellular level. PLoS ONE *5*, e13398.

Geoghegan, V., Stainton, K., Rainey, S.M., Ant, T.H., Dowle, A.A., Larson, T., Hester, S., Charles, P.D., Thomas, B., and Sinkins, S.P. (2017). Perturbed cholesterol and vesicular trafficking associated with dengue blocking in Wolbachia-infected Aedes aegypti cells. Nat. Commun. *8*, 526.

Giraldo-Calderón, G.I., Emrich, S.J., MacCallum, R.M., Maslen, G., Dialynas, E., Topalis, P., Ho, N., Gesing, S., Madey, G., Collins, F.H., and Lawson, D.; VectorBase Consortium (2015). VectorBase: an updated bioinformatics resource for invertebrate vectors and other organisms related with human diseases. Nucleic Acids Res. *43*, D707–D713.

Gustavsson, J., Parpal, S., Karlsson, M., Ramsing, C., Thorn, H., Borg, M., Lindroth, M., Peterson, K.H., Magnusson, K.-E., and Strålfors, P. (1999). Localization of the insulin receptor in caveolae of adipocyte plasma membrane. FASEB J. *13*, 1961–1971.

Haqshenas, G., Wu, J., Simpson, K.J., Daly, R.J., Netter, H.J., Baumert, T.F., and Doerig, C. (2017). Signalome-wide assessment of host cell response to hepatitis C virus. Nat. Commun. *8*, 15158.

Hedges, L.M., Brownlie, J.C., O'Neill, S.L., and Johnson, K.N. (2008). Wolbachia and virus protection in insects. Science *322*, 702–702.

Ikeya, T., Broughton, S., Alic, N., Grandison, R., and Partridge, L. (2009). The endosymbiont Wolbachia increases insulin/IGF-like signalling in Drosophila. Proc. Biol. Sci. *276*, 3799–3807.

Kambris, Z., Cook, P.E., Phuc, H.K., and Sinkins, S.P. (2009). Immune activation by life-shortening Wolbachia and reduced filarial competence in mosquitoes. Science *326*, 134–136.

Kasuga, M., Hedo, J.A., Yamada, K.M., and Kahn, C.R. (1982). The structure of insulin receptor and its subunits. Evidence for multiple nonreduced forms and a 210,000 possible proreceptor. J. Biol. Chem. *257*, 10392–10399.

Kumar, R., Agrawal, T., Khan, N.A., Nakayama, Y., and Medigeshi, G.R. (2016). Identification and characterization of the role of c-terminal Src kinase in dengue virus replication. Sci. Rep. *6*, 30490.

McMeniman, C.J., Lane, A.M., Fong, A.W., Voronin, D.A., Iturbe-Ormaetxe, I., Yamada, R., McGraw, E.A., and O'Neill, S.L. (2008). Host adaptation of a Wolbachia strain after long-term serial passage in mosquito cell lines. Appl. Environ. Microbiol. *74*, 6963–6969.

McMeniman, C.J., Lane, R.V., Cass, B.N., Fong, A.W., Sidhu, M., Wang, Y.-F., and O'Neill, S.L. (2009). Stable introduction of a life-shortening Wolbachia infection into the mosquito Aedes aegypti. Science *323*, 141–144.

Molloy, J.C., Sommer, U., Viant, M.R., and Sinkins, S.P. (2016). Wolbachia modulates lipid metabolism in Aedes albopictus mosquito cells. Appl. Environ. Microbiol. *82*, 3109–3120.

Moreira, L.A., Iturbe-Ormaetxe, I., Jeffery, J.A., Lu, G., Pyke, A.T., Hedges, L.M., Rocha, B.C., Hall-Mendelin, S., Day, A., Riegler, M., et al. (2009). A Wolbachia symbiont in Aedes aegypti limits infection with dengue, Chikungunya, and Plasmodium. Cell *139*, 1268–1278.

Nene, V., Wortman, J.R., Lawson, D., Haas, B., Kodira, C., Tu, Z.J., Loftus, B., Xi, Z., Megy, K., Grabherr, M., et al. (2007). Genome sequence of Aedes aegypti, a major arbovirus vector. Science *316*, 1718–1723.

O'Neill, S.L. (2018). The Use of Wolbachia by the World Mosquito Program to Interrupt Transmission of Aedes aegypti Transmitted Viruses. Adv. Exp. Med. Biol. *1062*, 355–360.

Paradkar, P.N., Duchemin, J.-B., Rodriguez-Andres, J., Trinidad, L., and Walker, P.J. (2015). Cullin4 is pro-viral during West Nile virus infection of Culex mosquitoes. PLoS Pathog. *11*, e1005143.

Parpal, S., Karlsson, M., Thorn, H., and Strålfors, P. (2001). Cholesterol depletion disrupts caveolae and insulin receptor signaling for metabolic control via insulin receptor substrate-1, but not for mitogen-activated protein kinase control. J. Biol. Chem. *276*, 9670–9678.

Peleg, J. (1968). Growth of arboviruses in monolayers from subcultured mosquito embryo cells. Virology *35*, 617–619.

Reed, L.J., and Muench, H. (1938). A simple method of estimating fifty per cent endpoints. Am. J. Epidemiol. *27*, 493–497.

Schultz, M.J., Tan, A.L., Gray, C.N., Isern, S., Michael, S.F., Frydman, H.M., and Connor, J.H. (2018). *Wolbachia w*Stri Blocks Zika Virus Growth at Two Independent Stages of Viral Replication. MBio *9*, e00738-18.

Shaw, W.R., Marcenac, P., Childs, L.M., Buckee, C.O., Baldini, F., Sawadogo, S.P., Dabiré, R.K., Diabaté, A., and Catteruccia, F. (2016). Wolbachia infections in natural Anopheles populations affect egg laying and negatively correlate with Plasmodium development. Nat. Commun. *7*, 11772.

Terradas, G., and McGraw, E.A. (2017). Wolbachia-mediated virus blocking in the mosquito vector Aedes aegypti. Curr. Opin. Insect Sci. *22*, 37–44.

Terradas, G., Joubert, D.A., and McGraw, E.A. (2017). The RNAi pathway plays a small part in Wolbachia-mediated blocking of dengue virus in mosquito cells. Sci. Rep. *7*, 43847.

Thomas, S., Verma, J., Woolfit, M., and O'Neill, S.L. (2018). Wolbachia-mediated virus blocking in mosquito cells is dependent on XRN1-mediated viral RNA degradation and influenced by viral replication rate. PLoS Pathog. *14*, e1006879.

Vainio, S., Heino, S., Månsson, J.E., Fredman, P., Kuismanen, E., Vaarala, O., and Ikonen, E. (2002). Dynamic association of human insulin receptor with lipid rafts in cells lacking caveolae. EMBO Rep. *3*, 95–100.

van den Hurk, A.F., Hall-Mendelin, S., Pyke, A.T., Frentiu, F.D., McElroy, K., Day, A., Higgs, S., and O'Neill, S.L. (2012). Impact of Wolbachia on infection with chikungunya and yellow fever viruses in the mosquito vector Aedes aegypti. PLoS Negl. Trop. Dis. *6*, e1892.

Voronin, D., Tran-Van, V., Potier, P., and Mavingui, P. (2010). Transinfection and growth discrepancy of Drosophila Wolbachia strain wMel in cell lines of the mosquito Aedes albopictus. J. Appl. Microbiol. *108*, 2133–2141.

Walker, T., Johnson, P.H., Moreira, L.A., Iturbe-Ormaetxe, I., Frentiu, F.D., McMeniman, C.J., Leong, Y.S., Dong, Y., Axford, J., Kriesner, P., et al. (2011). The wMel Wolbachia strain blocks dengue and invades caged Aedes aegypti populations. Nature *476*, 450–453.

Wen, Z., Gulia, M., Clark, K.D., Dhara, A., Crim, J.W., Strand, M.R., and Brown, M.R. (2010). Two insulin-like peptide family members from the mosquito Aedes aegypti exhibit differential biological and receptor binding activities. Mol. Cell. Endocrinol. *328*, 47–55.

WilsonWilson, H.L., Tran, T., Druce, J., Dupont-Rouzeyrol, M., and Catton, M. (2017). A neutralization assay for Zika and Dengue viruses using a real-time PCR-based endpoint assessment. J. Clin. Microbiol. *55*, 3104–3112.

Wu, M., Sun, L.V., Vamathevan, J., Riegler, M., Deboy, R., Brownlie, J.C., McGraw, E.A., Martin, W., Esser, C., Ahmadinejad, N., et al. (2004). Phylogenomics of the reproductive parasite Wolbachia pipientis wMel: a streamlined genome overrun by mobile genetic elements. PLoS Biol. *2*, E69.

Ye, Y.H., Woolfit, M., Rancès, E., O'Neill, S.L., and McGraw, E.A. (2013). Wolbachia-associated bacterial protection in the mosquito Aedes aegypti. PLoS Negl. Trop. Dis. *7*, e2362.

Ye, Y.H., Ng, T.S., Frentiu, F.D., Walker, T., van den Hurk, A.F., O'Neill, S.L., Beebe, N.W., and McGraw, E.A. (2014). Comparative susceptibility of mosquito populations in North Queensland, Australia to oral infection with dengue virus. Am. J. Trop. Med. Hyg. *90*, 422–430.

Zhang, G., Asad, S., Khromykh, A.A., and Asgari, S. (2017). Cell fusing agent virus and dengue virus mutually interact in Aedes aegypti cell lines. Sci. Rep. *7*, 6935.

STAR★METHODS

KEY RESOURCES TABLE

REAGENT or RESOURCE	SOURCE	IDENTIFIER
Antibodies		
InsR-pY1189 Antibody (IR phosphor-specific antibody)	Kinexus, Canada	Cat#AB-PK663
Mouse monoclonal anti-Actin antibody	Abcam	Cat#ab3280
Bacterial and Virus Strains		
Wolbachia strain wMel	Scott O'Neill (Monash University); Moreira et al., 2009	N/A
DENV (type 2) strain East Timor (ET-300)	Andrew van der Hurk; Ye et al., 2014	N/A
ZIKV strain Cambodia (2010)	Nikos Vasilakis (University of Texas Medical Branch, Galveston, USA); Duchemin et al., 2017	N/A
ZIKV Strain Puerto-Rico (2016)	Nikos Vasilakis (University of Texas Medical Branch, Galveston, USA); Buchman et al., 2018	N/A
Chemicals, Peptides, and Recombinant Proteins		
HNMPA-(AM)3	Santa Cruz Biotechnology	Cat#sc-221730
RNAiMAX Lipofectamine	Invitrogen	Cat#1756083
TaqMan Fast Virus 1-step Master Mix	ThermoFisher Scientific	Cat#4444432
Taqman Fast Advanced Master Kit (Applied Biosystems)	ThermoFisher Scientific	Cat#4444557
Critical Commercial Assays		
Kinexus Antibody Microarray	Kinexus, Canada	Cat#KAM-900P
Experimental Models: Cell Lines		
Aag2 cells	Scott O'Neill (Monash University); Terradas et al., 2017	N/A
Vero cells	Julian Druce (University of Melbourne); Wilson et al., 2017	N/A
Experimental Models: Organisms/Strains		
Mosquitoes strain- Brisbane	Ary Hoffmann (University of Melbourne); Duchemin et al., 2017	N/A
Mosquitoes strain- Higgs	Omar S Akbari (University of California San Diego); Buchman et al., 2018	N/A
Oligonucleotides		
Primers for siRNA experiments: See Table S2	This paper	N/A
Software and Algorithms		
Prism 7	GraphPad Software, La Jolla CA (USA)	https://www.graphpad.com/
GNU Image Manipulation Program (GIMP) 2.10.8	Open source	https://www.gimp.org/news/2018/11/08/gimp-2-10-8-released/
Image lab software	BioRad, Hercules CA (USA)	https://www.bio-rad.com/en-au/product/image-lab-software?ID=KRE6P5E8Z
ImageQuant TL software	GE Healthcare Life Sciences	N/A

CONTACT FOR REAGENT AND RESOURCE SHARING

Further information and requests for resources and reagents should be directed to and will be fulfilled by the Lead Contact, Christian Doerig (christian.doerig@monash.edu).

EXPERIMENTAL MODEL AND SUBJECT DETAILS

Mosquito cell lines

The immune-competent *Aedes aegypti* cell line Aag2 (Fallon and Sun, 2001; Peleg, 1968) chronically infected with *Wolbachia's* strain *w*Mel (denoted as Aag2*w*Mel) was created previously (Terradas et al., 2017). A *Wolbachia*-free control line (Aag2*w*Mel.tet) was obtained after three successive passages in the presence of 10 μg/ml tetracycline (Terradas et al., 2017). Both cell lines were examined for the presence of *Wolbachia* using Fluorescent *In Situ* Hybridization (FISH) (Voronin et al., 2010) and quantitative PCR (qPCR) methods (McMeniman et al., 2008) as previously reported. The Aag2*w*Mel line was shown to be highly-infected with *Wolbachia* and Aag2wMel.tet was shown to be *Wolbachia* free (Figure S4). Both cell types were routinely passaged in filtered complete media: a 1:1 mixture of Schneider's media (Life Technologies) and Mitsuhashi-Maramorosch, supplemented with 10% heat-inactivated FBS (Life Technologies) and 1% Penicillin/Streptomycin (Life Technologies). Cells were reared in a non-humidified incubator at 25°C.

Mosquitoes

We used female mosquitoes of the Higgs and Brisbane strains (kindly provided by Dr. Ary Hoffmann, University of Melbourne, Australia, and Dr Akbari, University of California, respectively).

METHOD DETAILS

Kinexus™ antibody microarray

Using the Kinexus™ KAM-900 spanning 895 pan-specific and phosphosite antibodies (see Table S1), microarray analysis was performed with a single biological sample for each condition as described (Haqshenas et al., 2017). Aag2*w*Mel and Aag2*w*Mel.tet cells were gown to 90% confluence in 175 cm^2 flasks. Cells were harvested, washed twice with 10 mL phosphate-buffered saline (PBS), pelleted at 200x g and sent on dry ice to Kinexus for microarray analysis as described (Haqshenas et al., 2017). To each cell pellet, 600 μl lysis buffer was added and sonicated 4 times at 10 s before they were subjected to ultracentrifugation at 50,000 rpm for 30 minutes. Using the Bradford assay, the protein concentrations were 17.07 mg/ml and 15.10 mg/ml for *Wolbachia*-free and infected cells, respectively. 100 μg of protein was loaded onto each microarray.

Signals from the array that warrant further analysis are distributed into two categories (Page 2 of the Excel spreadsheet in Table S1). Category (1): PRIORITY list, which contains cell factors that meet the following selection criteria: (i) %Change Fold to Control (CFC) $\geq$ 75; (ii) SUM of %Error Ranges < 0.75 x %CFC value; (iii) at least one Globally Normalized intensity value $\geq$ 1500; Category (2): POSSIBLE list, which contains cell factors that meet the following criteria: (i) %CFC $\geq$ 50; (ii) SUM of %Error Ranges < 0.85 x % CFC value; (iii) at least one Globally Normalized intensity value $\geq$ 1000. The Kinexus antibodies recognize human proteins which share various levels of homology with their mosquito orthologs. The sequences of the epitopes which are recognized by the Kinexus antibody microarray are available on the Kinexus website (http://www.kinexus.ca). We used NCBI blast to determine if an epitope recognized by the Kinexus antibody was conserved in mosquito proteins.

Selection of candidate genes and their targeting with siRNA and small molecules

One cellular kinase, IR, that was downregulated in the presence of *Wolbachia* infection in the Kinexus arrays, was selected for functional analysis (see Results). The *Ae. aegypti* IR gene (accession number AAEL002317-PA) shares (Giraldo-Calderón et al., 2015; Nene et al., 2007) high levels of similarity (80%) in its active site (amino acids 1016-1303, NCBI description of IR) with its human ortholog (accession number AAA59452.1) (Figure S1). The sequences of primers used to assess expression, and of siRNAs designed for the *Ae. aegypti* genes (manufactured by Sigma-Aldrich), are found in Table S2. We performed Blast searches of the siRNA sequences against the *Ae. aegypti* genome and the genome of the cell fusing agent virus (CFAV), an insect flavivirus which permanently infects Aag2 cells (Zhang et al., 2017), to ensure they did not match to any non-target genes.

To further validate the role of IR activity in virus replication, we used the small molecule HNMPA(AM)-3 (Hydroxy-2-naphthalenylmethylphosphonic Acid Trisacetoxymethyl Ester). The HNMPA(AM)-3 stock (100 mM) was prepared in DMSO. The toxicity of the compound was measured by PrestoBlue® Cell Viability Reagent (Thermo Fisher Scientific)(Haqshenas et al., 2017) and sub-toxic concentrations of each compound were used for the experiment where the effect of the compound was measured on DENV replication. Serial 2-fold dilutions of the inhibitor were prepared using the complete medium containing DMSO at concentration corresponding to 25 μM of the inhibitor. The complete medium containing the DMSO vehicle but no inhibitor was used as negative control in above experiments (Haqshenas et al., 2017).

Infection of live mosquitoes with ZIKV and treatment with the IR inhibitor

Eight to ten, 5-8 day old female mosquitoes of the Higgs and Brisbane strains (kindly provided by Dr. Ary Hoffmann, University of Melbourne, Australia, and Dr Akbari, University of California, respectively), were starved the day before being challenged with an virus-infected blood meal containing $10^{5.6}$ $TCID_{50}$ (50 percent tissue culture infectious dose)/mL, through membrane feeding using chicken blood and skin (Paradkar et al., 2015). Chicken blood and skin were provided by the Small Animal Facility of the Australian Animal Health Laboratory from chicken bred in the laboratory with no sign of arboviral infection. The procedure was conducted with approval from AAHL Animal Ethics Committee. The blood was spiked with ZIKV just before mosquito blood-feeding, with or without

IR inhibitor. After one hour, the mosquitoes were anesthesized with CO_2 and blood-fed females were sorted and kept in a 200 mL cardboard cup at 27.5°C, 65% humidity and 14:10 day:night photoperiod. The blood-fed mosquitoes were kept for 7 days with 10% sugar solution provided *ad libitum*.

siRNA transfection

This was done as described previously (Terradas et al., 2017). Aag2*w*Mel and Aag2*w*Mel.tet cells were seeded the day before transfection in a flat bottom Greiner 96-well plate (Sigma-Aldrich) at 70%–80% confluence. The following day, two different treatments were applied to the cells in a serum-free environment: Scrambled siRNA and IR siRNA (Table S2). All siRNA treatments were performed using Lipofectamine RNAiMAX (Sigma-Aldrich) reagent according to manufacturer's protocol.

Immunoblot analysis

Samples were prepared and resolved onto a 4%–12% polyacrylamide gel (Haqshenas et al., 2017). The pan- and phosphosite-specific (recognizing IR pY1189) antibodies were purchased from the Kinexus, and diluted 1/2000 in blocking buffer (5% skim milk or BSA in Tris-buffered saline, pH 7.5, 0.05% Tween 20). The blots were maintained in the blocking buffer for 4-5 h at room temperature before they were exposed to the diluted primary antibodies at 4°C overnight. The HRP-conjugated, anti-rabbit and mouse secondary antibodies were purchased from Monash Antibody Technologies Facility (MATF, Melbourne, Australia) and diluted 1/30000 and 1/20000, respectively, in 0.5x blocking solutions before adding them to the membranes. The bound secondary antibodies were detected using the Amersham ECL Prime Western Blotting Detection Reagent (GE Healthcare). Actin was detected as described previously (Haqshenas et al., 2017), and all signals were normalized to actin levels.

DENV and ZIKV infection and quantification

In vitro infections were performed 16-18h post-transfection with siRNA. Cells were washed with PBS before and after the virus inoculation at a DENV-2 Multiplicity of Infection (MoI) of 0.5, conditions in which blocking of viral super-infection was most clearly seen in our pilot studies (data not shown). ZIKV was used at MoI of 0.1, which showed the highest effect in the current study (see Results). The viral inoculum was removed 2h post-infection and cells were grown in complete media containing 2% FBS. Viral RNA was quantified 5 days post-infection by collection of 20 μl supernatant and mixed 1:1 with 20μl extraction buffer (1X Tris-EDTA, 0.1M EDTA, 1M NaCl and 2.5μl proteinase K). They were then incubated in a C1000Thermal Cycler (Bio-Rad, California USA) at 56°C for 5min, then 98°C for 5min. The samples were subsequently used for the absolute quantification of DENV-2 (Ye et al., 2014). The standard curves ranged from 10^8 to 10 DENV and ZIKV fragment copies. Virus load in each sample was extrapolated (genomic copies/ml) from the standard curves. For ZIKV, the standard curve was derived by serial dilution of virus and determining TCID50 equivalent Ct values, followed by extrapolation (TCID50 /ml equivalent) (Duchemin et al., 2017). The infectivity of supernatant fluids collected from siRNA-treated cells infected with DENV was determined as described previously (Duchemin et al., 2017), normalized to housekeeping gene rps17, and expressed as TCID50/ml. Briefly, 20 μl of supernatant fluids were collected at respective time points, and it was serially 10-fold diluted in medium (DMEM containing 2% FBS). Using 96-well plates, Vero cells at confluence of 50%–60% were infected with 30 μl of each dilution (5 replicates) for 2 h before the medium was removed, cell washed twice, and 100 μl fresh medium were added to each well. The cells were incubated for 6 days before they were observed for cytopathic effect (CPE). The 50% endpoint was calculated using the Reed and Muench method (Reed and Muench, 1938).

One-step quantitative reverse-transcription PCR (qRT-PCR) was performed using TaqMan® Fast Virus 1-step Master Mix (Roche) in a total 10 μl, following the manufacturer's instructions. The oligonucleotide primers and probe sequences used for the detection of ZIKV and DENV (Ye et al., 2014) are presented in Table S2. The thermal profile was as stated previously for qPCR analysis, with the addition of 10 min incubation RT step at 50°C followed by 20 s at 95°C for RT inactivation at the start of the run.

Taqman Fast Advanced Master Kit (Applied Biosystems) and specific oligonucleotides and probes (Table S2) were used to amplify the housekeeping rpS17 gene and *Wolbachia* DNA. The thermal cycles included one initial cycle at 50°C for 2 minutes and 95°C for 1 minute, followed by 50 cycles at 95°C for 5 s and 60°C for 1 minute.

DATA ANALYSIS

Immunoblot images were captured using the Image Lab™ software (BioRad) and analyzed by the ImageQuant TL software (GE Healthcare Life Sciences). The amino acid sequences of human proteins were extracted and blasted against *Ae. Aegypti* proteins. Images were labeled using the open-source GNU Image Manipulation Program (GIMP) version 2.10.8.

QUANTIFICATION AND STATISTICAL ANALYSIS

qPCR and RT-qPCR were carried out in duplicates. Multiple Unpaired, t test in GraphPad Prism7 software (GraphPad Software, Inc., La Jolla, CA) was used to determine significance of differences between siRNA-treated versus mock-treated controls. All ZIKV and DENV loads were reported on a log scale given the spread of values. The statistical significance of the data pertaining to mosquito infection (Figure 4) is assessed by a Student t test. ****$p < 0001$. Standard deviation is indicated for all other quantitated data.